Disturbed Resting Functional Inter-Hemispherical Connectivity of the Ventral Attentional Network in Alpha Band Is Associated with Unilateral Spatial Neglect

Tsutomu Sasaki[1*], Masayuki Abe[2], Eiichi Okumura[3], Toyoji Okada[4], Kimito Kondo[5], Kensuke Sekihara[6], Wataru Ide[7], Hajime Kamada[7]

1 Division of Occupational Therapy, School of Health Sciences, Faculty of Medicine, Shinshu University, Matsumoto, Japan, 2 Department of Occupational Therapy, Hokuto Hospital, Obihiro, Japan, 3 Department of MEG, Yokogawa Electric Corporation, Kanazawa, Japan, 4 Department of Clinical Laboratory Medical Technology, Hokuto Hospital, Obihiro, Japan, 5 Department of Neurology, Hokuto Hospital, Obihiro, Japan, 6 Department of Systems Design and Engineering, Tokyo Metropolitan University, Tokyo, Japan, 7 Department of Neurosurgery, Hokuto Hospital, Obihiro, Japan

Abstract

Unilateral spatial neglect (USN) is one of the most common symptoms of right hemisphere damage; its classical symptom is that patients fail to respond to information on their left side. It has been postulated that disturbance of 2 separate attentional networks relates to the occurrence of USN. However, little is known about the underlying mechanism and neuronal substrates. In this study, we measured spontaneous neural activity by means of magnetoencephalography in 13 patients with brain damage and 5 control subjects. To study the relationship between functional connectivity at rest and severity of USN symptoms, we determined the imaginary coherence values relating to the inter-hemispherical ventral and dorsal attentional networks, as well as the clinical severity of USN using neuropsychological tests and behavioral rating scales. The present results showed that inter-hemispherical connectivity in the ventral attentional network, especially between the left and right angular gyri, detected in the alpha band is associated with the severity of USN symptoms. This may suggest that connectivity of inter-hemispherical homologous regions of the ventral attentional network in the alpha band could be one of the biomarkers of attentional network imbalance occurring in patients with USN.

Introduction

There has been an increasing interest in understanding how the human brain works when it is at rest. In particular, the analysis of functional connectivity during rest and the associated temporal correlation of brain activities in different regions has become a popular topic of study. Abnormalities in the interactions of network components play critical roles in common neurological and psychiatric disorders such as epilepsy [1], depression [2], schizophrenia [3], dementia [4], and autism [5]. In addition, damage to specific functionally connected networks is known to lead to distinct types of cognitive dysfunction [6–9].

One of the most prominent symptoms of brain damage is unilateral spatial neglect (USN), which is well known as a common and disabling consequence of right-hemisphere damage. It is a complex syndrome characterized by a failure to attend to, look at, or respond to stimuli located on the side of the body opposite to the side of the affected hemisphere. Although a large number of studies on USN have been published, the neuronal substrates of USN are not well understood. USN occurs in about 25–30% of all stroke-affected individuals [10,11]. The most frequent sites of damage are the right temporoparietal junction [12] and the right inferior parietal [13–15], ventral frontal [16], and superior temporal gyri [17]. However, unilateral damage to subcortical regions such as the thalamus [18–20], striatum, internal capsule [20], putamen, caudate nucleus, pulvinar [21], and cerebellar region [22] have been reported to cause USN symptoms. These findings imply that structural damage of specific focal brain regions cannot

fully explain the neural mechanisms underlying USN, leading to the idea that USN may be better explained by the dysfunction of distributed cortical networks that control attention [23–25].

With the recent development of brain imaging techniques, the neural mechanisms of USN have been examined from the viewpoint of brain networks implicated in the control of attention. It has been suggested that 2 attentional systems exist in the human brain: the ventral attentional network (VAN) and dorsal attentional network (DAN) [24–27]. The VAN includes the inferior frontal gyrus, ventral frontal gyrus (VFG), supramarginal gyrus (SMG), angular gyrus (AG), and superior temporal gyrus, while the DAN includes superior frontal gyrus (SFG), superior parietal lobule, and middle temporal gyrus. In most cases with USN, lesions appear to cluster around a large perisylvian network in the right hemisphere [12,23,28]. Using diffusion tensor imaging tractography, Urabanski et al. [29] identified that damage to clusters in the perisylvian white matter lead to USN. He et al. [30] demonstrated that disrupted functional connectivity in the VAN is manifested in cases of USN, especially during the acute phase. With respect to the DAN, it has been reported that functional connectivity between inter-hemispheric homologous regions in the DAN, under task-driven conditions [30,31], as well as under resting conditions [32], is associated with USN symptoms.

The majority of studies demonstrating a relationship between functional connectivity and USN symptoms have employed functional magnetic resonance imaging (MRI). An important limitation of this technique is that it measures slow fluctuations in the blood oxygen level dependent signal, an indirect measure of neural activity in the brain [33]. On the other hand, electroencephalography and magnetoencephalography (MEG) directly measure electrophysiological brain activity. Furthermore, the high temporal resolution of electroencephalography and MEG allow for the separation of neuronal activity into oscillatory components that reflect distinct biophysical properties [34]. In fact, several studies have revealed relationships between neural oscillation and brain function [35–37]. However, to the best of our knowledge, no study to date has directly measured both neural activity and functional connectivity in patients with USN. The purpose of the present study was to 1) use MEG to measure neural activity in patients with USN during rest and 2) evaluate the relationship between functional connectivity and USN severity.

Materials and Methods

Subjects

Thirteen stroke patients with right-hemisphere damage (mean age 65.1 ± 11.8 (years ± SD) in the range of 38–82 years; 7 men and 6 women) and 5 healthy volunteers (mean age 26.0 ± 1.3 (years ± SD) in the range of 25–28 years; 3 men and 2 women) participated in this study. The demographic and clinical characteristics of the participants are summarized in Table 1. All patients received standard therapy at the stroke unit during the acute phase and individually tailored multidisciplinary rehabilitation programs during the subacute, recovery, and chronic phases. All were right-handed as assessed by the Edinburgh Inventory [38]. Subjects were in

Table 1. Clinical data.

| | | | | | Months | | USN | BIT | |
| | | | | | from | | Index | 3 types | CBS |
Case	Sex	Age	LQ	Etiology	onset	MMSE	(/96)	(/66)	(/30)
USN(+) 1	M	73	100	Inf	8	21	42	39	3
USN(+) 2	W	78	100	Inf	9	15	56	44	12
USN(+) 3	M	82	82	Inf	1	13	36	26	10
USN(+) 4	M	38	100	Hemo	2	17	29	24	5
USN(+) 5	W	79	80	Inf	4	23	35	25	10
USN(+) 6	W	65	100	Inf	4	25	12	9	3
USN(+) 7	W	63	100	Inf	3	29	16	1	15
USN(+) 8	M	71	100	Inf	1	29	5	1	4
USN(-) 1	M	56	100	Inf	1	29	0	0	0
USN(-) 2	W	60	100	Hemo	1	24	0	0	0
USN(-) 3	M	50	100	Inf	2	27	0	0	0
USN(-) 4	W	65	100	Inf	3	29	0	0	0
USN(-) 5	M	66	100	Hemo	4	27	0	0	0
Normal 1	W	25	98	-	-	30	0	0	0
Normal 2	M	25	100	-	-	30	0	0	0
Normal 3	M	27	100	-	-	30	0	0	0
Normal 4	W	25	99	-	-	30	0	0	0
Normal 5	M	28	100	-	-	30	0	0	0

Inf: infarction; Hemo: hemorrhage; LQ: Laterality Quotient ; MMSE: Mini-Mental State Examination ; BIT: Behavioural Inattention Test ; CBS: Catherine Bergego Scale .

good health and had no history of neurological or psychiatric disease. The present study was conformed to the ethical principles of the Helsinki Declaration, and approved by the Ethics Committee of Shinshu University and by the Ethics Committee of Hokuto Hospital. Written informed consent was obtained from each subject.

Clinical assessment

All subjects were evaluated by means of the following 4 neuropsychological tests: i) the Mini-Mental State Examination scored from 0 (severe) to 30 (mild) [39], ii) the Star Cancellation in the Behavioural Inattention Test (BIT) [40] scored from 0 (mild) to 54 (severe), iii) the Daisy Copying (BIT) scored from 0 (mild) to 3 (severe), iv) the Line Bisection (BIT) scored from 0 (mild) to 9 (severe). All subjects were also scaled on their behavioral attentional disturbance in daily living using the Catherine Bergego Scale (CBS) scored from 0 (mild) to 30 (severe) [41]. To confirm whether subjects exhibit USN and to measure the severity of USN, we defined the USN index as the total score of the Star cancellation, the Daisy Copying, the Line Bisection, and the CBS tests, which totally ranges from 0 (mild) to 96 (severe). To control for the impact of right hemisphere damage per se, subjects with brain damage were classified into USN(+) and USN(-) on the basis of the USN index: USN(+) if the USN index is above 0, USN(-) if the index scores 0. As shown in Table 1, USN symptoms were evident in 8 out of the 13 patients with brain damage. Subjects were analyzed in 3 groups: 1) Normal controls; 2) USN(-) patients

with brain damage but no USN symptoms; and 3) USN(+) patients with brain damage and USN symptoms.

Structural MRI

Imaging data were acquired on a Signa 3.0 Tesla system (GE Healthcare). High-resolution structural images were acquired with a three-dimensional fast spoiled gradient-recalled-echo T1-weighted sequence (repetition time: 9.5 msec; echo time: 3.9 msec; flip angle: 13°; field of view: 240 mm; slice thickness: 1.6 mm; matrix: 288 × 288; 128 slices). For patients with stroke, we drew lesion overlap maps from the T1-weighted images (Figure 1). Lesion extent was determined for each patient by selecting brain scans that showed the greatest extent of damage and drawing the lesion borders directly onto the original images, using the MRIcron software [42] available online (http://www.nitrc.org/projects/mricron). All lesion maps were double-checked by a neurologist or a therapist trained to read brain scans.

MEG recording

Magnetic fields were measured in a 160-channel whole-head-type gradiometer system (MEGvision PQA1160C; Yokogawa Electric Corporation, Japan). MEG data were sampled at 1000 Hz per channel (band pass 0.16–200 Hz and notch 50 Hz) with the subjects in a supine position with eyes closed for 10 minutes. During the MEG recordings, subjects were instructed to close their eyes and reduce eye movements, but to remain awake as much as possible. During the recordings, the investigator and MEG technician checked the on-line signal for visual signs of drowsiness (e.g., slow eye movement activity) and observed the patients using a video monitor. Each subject's head position relative to the sensor array was determined before and after the MEG recording.

Data analysis

General. Data were analyzed using Matlab 7.13 (MathWorks, Natick, MA) and custom scripts for general technical computing and source reconstruction, the FieldTrip open source Matlab toolbox [43] (http://www.ru.nl/fcdonders/fieldtrip) for functional connectivity analysis, component analysis, SPM8 (Wellcome Department of Cognitive Neurology, London, UK, http://www.fil.ion.ucl.ac.uk/spm/software/spm8/) for spatial normalization, and Statistics toolbox 7.6 (MathWorks, Natick, MA) for statistical analysis. The SPSS 17.0 was also used for statistical analysis.

Preprocessing. First, MEG data were subjected to principle component analysis (PCA) and typical noise components (e.g. magnetized metal artifacts) were removed using visual inspection. After that, we defined trials of interest from the continuous MEG data. Trials were defined as continuous data segments of two-second frame length in steps of 1 second, excluding trials with magnetic flux in any channel that exceeded 2000 fT. The number of analyzed trials, 140 trials, was equalized among subjects.

Region of interest and network nodes. For functional connectivity analysis, first, we selected 16 regions of interest (ROIs) involved in attentional networks based on the previous studies [24–27,30–32]: the DAN consisting both the SFG,
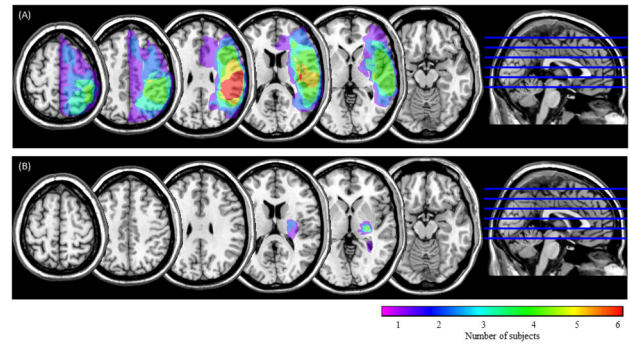

Figure 1. Lesion overlap maps. USN(+) group (A) and USN(-) group (B). Horizontal sections through a template brain show the frequency of damage for each voxel. The color scale indicates the increasing frequency of overlapping lesions from violet (n = 1) to red (n = 6).
doi: 10.1371/journal.pone.0073416.g001

superior parietal lobule, and middle temporal region, and the VAN consisting of both the VFG, the inferior frontal gyrus, the SMG, the AG, and the superior temporal gyrus. Secondly, these 16 ROIs were spatially normalized according to the Montreal Neurological Institute coordinate system, and the structural volumes of ROIs were obtained using WFU-PickAtlas 3.0.3 software (ANSIR Laboratory, Wake Forest University School of Medicine) [44,45]. The ROI labels used were from the automated anatomical labeling atlas of 116 segmented structures [46]. Finally, the nodes were generated by means of down-sampling these ROI three-dimensional images from 2-mm to 10-mm spacing. 388 nodes in 16 ROIs were obtained. The number and position of nodes in each ROI is summarized in Table S1 and Figure S1, respectively.

Source-space coherence analysis. Coherence is a widely used representative measure, and we adopted the imaginary part of coherence (imaginary coherence; IC) to remove the spurious coherence caused by leakage associated with our imaging algorithm [47,48]. IC exploits the fact that phase similarities among time series arising from a common reference or volume conduction occur with zero time delay. Thus, by omitting the real component of coherence, which mostly contains similarities with zero time lag, we removed suspect associations. By limiting our analysis to the IC, our goal was to reveal only true interactions between brain areas occurring with a certain time lag [49].

Source-space coherence analysis was performed the following procedure. First, the node locations on individual MRI coordinates were generated by using predefined ROIs (Table S1 and Figure S1) and the warping parameters calculated by SPM8 with MRI-T1 template and individual MRI-T1 images. Seconds, the time course for each node was calculated by adaptive spatial filtering [50], using a single spherical volume conductor model based on the individual MRI T1-image. To avoid potential de-ranking after PCA noise rejection, we performed the Tikonov regularization for the covariance matrix [51,52]. Next, IC of all node combinations were calculated using Fourier transform with Hanning window. The absolute
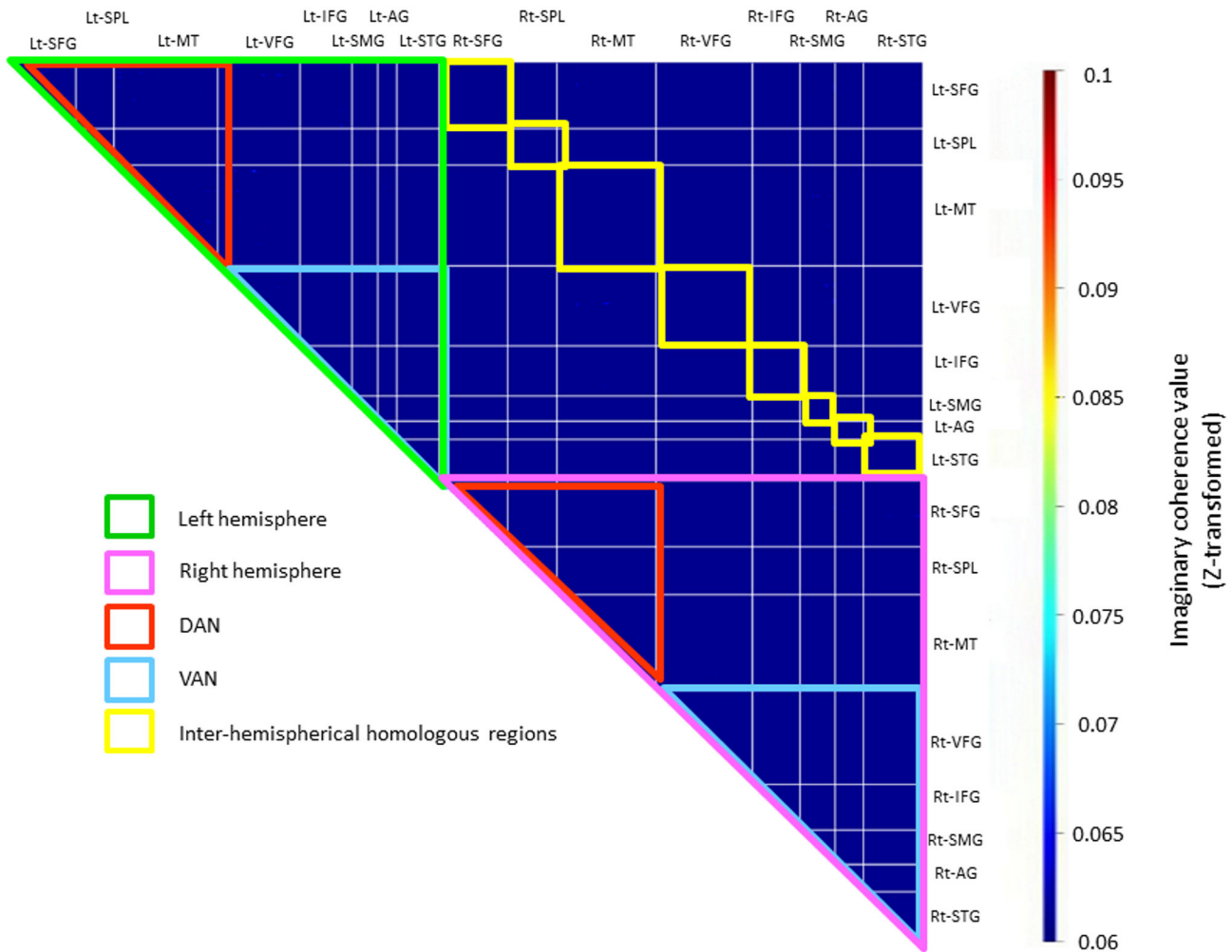
Figure 2. Illustration of IC matrix. The color scale indicates magnitude of imaginary coherence (Z-transformed). Area surrounded by green dashed line, and by pink dashed line indicates IC of left hemisphere and right hemisphere, respectively. Area surrounded by red dashed line and by blue dashed line indicates IC of the DAN and the VAN, respectively. Yellowed areas indicate inter-hemispherical homologous regions. SFG: superior frontal gyrus; SPL: superior parietal lobule; MT: middle temporal region; VFG: ventral frontal gyrus; IFG: inferior frontal gyrus; SMG: supramarginal gyrus; AG: angular gyrus; STG: superior temporal gyrus.
doi: 10.1371/journal.pone.0073416.g002

value of IC was used rather than coherency because we were interested in the magnitude of connectivity at each voxel rather than in the directionality of the information flow [53]. Then, we calculated average coherence for 6 frequency bands: delta, 1–4 Hz; theta, 4–8 Hz; alpha, 8–13 Hz; beta, 13–30 Hz; low gamma, 30–50 Hz; and high gamma, 50–100 Hz [27,54–57]. The connectivity (that is, IC) at each frequency of interest was estimated by averaging across all its Fisher's Z-transformed (arctanh(IC); the inverse hyperbolic tangent of IC) connections [47]. Then we obtained individual subjects' IC matrices and grand-averaged (on Z-transformed space) IC matrices across subjects for each group (see Figure 2). Finally, the ROI IC values were calculated for each subject by averaging across voxel pairs within each ROI. These ROI IC values were used for correlation analysis between IC and USN index.

Correlation between IC and USN index. To determine whether functional connectivity predicts clinical severity of USN, we performed regression analysis. In this analysis, normal controls were excluded to reveal the influence of brain damage on functional connectivity relating to USN symptom more clearly.

Results

IC among groups at each frequency band

Figure 3 showed that the IC matrices among groups in the delta and theta band were strikingly similar. For these bands, the USN(-) group seemed to exhibit higher connectivity between the left DAN/left VAN and between the /left/right hemisphere than did the other 2 groups (Figure 3a, 3b).

ANOVA revealed, however, that no statistical difference was found among groups for the comparison between the left DAN and the left VAN ($F_{2,15}$ = 2.828, p > 0.1 for delta band: $F_{2,15}$ = 2.914, p > 0.1 for theta band), and between left hemisphere and right hemisphere ($F_{2,15}$ = 1.407, p > 0.1 for delta band: $F_{2,15}$ = 1.099, p > 0.1 for theta band). The matrices among groups in the beta band and low-/high gamma band were also similar. For these 3 bands, each group seemed to exhibit lower connectivity than in other oscillatory bands (Figure 3d, 3e, 3f). The patterns of IC maps in the alpha band seemed to be considerably different from that of other frequency bands. Each group exhibited different IC pattern. For normal group, IC within right hemisphere seemed to be higher than within left hemisphere, however, statistical analysis showed no difference (t(8) = -1.699, p > 0.1). For the USN(-) group, although IC within left hemisphere seemed to be higher IC than within right hemisphere, no statistical difference was found(t(8) = -0.648, p > 0.1). For the USN(+) group, IC within left hemisphere seemed to be higher than within right hemisphere, however, no statistical difference was found (t(14) = 0.740, p > 0.1) (Figure 3c).

Based on previous findings [30–32], which suggested connectivity between inter-hemispherical homologous regions in attentional networks, our goal was to determine whether inter-hemispherical connectivity between homologous regions in the DAN as well as in the VAN (e.g., left and right SFG) contribute to USN symptoms.

For the delta band, ANOVA revealed statistically different IC between the left and right SFG among the groups ($F_{2,15}$ = 4.764, p < 0.05). Post hoc analysis confirmed that the USN(+) group exhibited greater IC than the normal group (uncorrected p < 0.05). The IC between the left and right VFG also showed significantly different patterns among the groups ($F_{2,15}$ = 3.964, p < 0.05). Post hoc comparison confirmed that compared to the normal group, the USN(+) group exhibited greater IC (uncorrected p < 0.05). In the theta and beta bands, no differences between inter-hemispherical homologous regions were found among the groups. For the alpha band, there was a significant difference between the left/right AG among groups ($F_{2,15}$ = 5.105, p < 0.05), and post hoc comparisons confirmed that the USN(+) group showed lower IC than the USN(-) group (uncorrected p < 0.05), not but compared to the normal group (Figure 4a). We also compared IC between the left and right VAN, as well as between the left and right DAN, in the alpha band among the groups. Analysis showed a statistical difference among the groups for the VAN ($F_{2,87}$ = 5.566, p < 0.01), and post hoc comparisons confirmed that compared to the USN(-) group, the USN(+) group showed lower IC (uncorrected p < 0.01) but no difference was found between the USN(+) group and the normal group (uncorrected p > 0.05) (Figure 4b), while for the DAN, there was no statistical difference among groups ($F_{2,51}$ = 0.034, p > 0.10) (Figure 4c). For the gamma band, ANOVA revealed a significant difference among groups in the IC between the left and right AG in the lower range (30–50 Hz) ($F_{2,15}$ = 4.227, p < 0.05) and between the left and right SMG in the higher range (50–100 Hz) ($F_{2,15}$ = 4.404, p < 0.05). Post hoc comparisons confirmed that the USN(+) group exhibited lower IC than the USN(-) group in both

ranges (each at uncorrected p < 0.05). We also calculated IC of the inter-hemispherical attentional network for the low-gamma band. Analysis revealed a statistical difference among the groups for the VAN ($F_{2,87}$ = 6.045, p < 0.01), and post hoc comparisons confirmed that compared to the USN(-) group, the USN(+) group showed lower IC (uncorrected p < 0.01), while for the DAN, there was no statistical difference among groups ($F_{2,51}$ = 0.949, p > 0.10).

Correlation between IC and USN index

To determine whether the connectivity between inter-hemispherical homologous regions in attentional networks predicts USN severity, we performed regression analysis. For the delta band, a significant correlation was found between the connectivity of the left/right SFG and USN index (F(1,11) = 10.773, p = 0.007, r^2 = 0.495). For the theta band, no significant relation was found. For the alpha band, a significant correlation was found for the left/right AG and USN index (F(1,11) = 11.597, p = 0.006, r^2 = 0.513) (Figure 5). We also performed regression analysis for the DAN and VAN in the alpha band, demonstrating that correlation between the VAN and USN index showed a trend for significance (F(1,11) = 4.403, p = 0.058, r^2 = 0.286), while correlation in the DAN did not reach significant level (F(1,11) = 1.442, p = 0.255, r^2 = 0.116) (Figure 5). For other frequency bands, i.e., the beta band, the low-gamma band, and the high-gamma band, no significant relation was found excepting the relation between the IC of the left/right STG and USN index in the high-gamma band (F(1,11) = 5.290, p = 0.04, r^2 = 0.325).

Discussion

This is the first report demonstrating a relationship between MEG measures of resting-state functional connectivity in specific oscillatory bands and clinical symptoms in patients with USN. Carter et al. [32] previously reported a relationship between resting functional connectivity and USN symptoms, in which inter-hemispherical functional connectivity predicted USN symptoms. However, they did not shed light on the relevance of their results to different frequencies of neural oscillation. Furthermore, they did not implicate the VAN in their findings. We have extended their results by demonstrating that patient with USN had lower inter-hemispheric connectivity in the alpha band for the VAN, especially the AG, and that IC value for these regions was correlated with severity of USN.

Two attentional networks, the DAN and VAN, are thought to be functionally heterogeneous, but to interact with each other. The DAN is involved in shifting and maintaining attention [58], goal-directed stimulus, and response selection [59] and contains visuotopic maps of contralateral space [60]. The DAN is usually intact in patients with USN [61,62]. On the other hand, the VAN is damaged in a majority of patients with neglect [61,62], and appears to be specialized for redirecting the DAN to novel and behaviorally relevant stimuli [31]. The VAN is also involved in non-spatial processes such as vigilance [63] as well as detection [64,65]. Direct damage of ventral regions, such as that observed in most of the patients in this study, causes a malfunctioning of non-spatial processes and abnormal

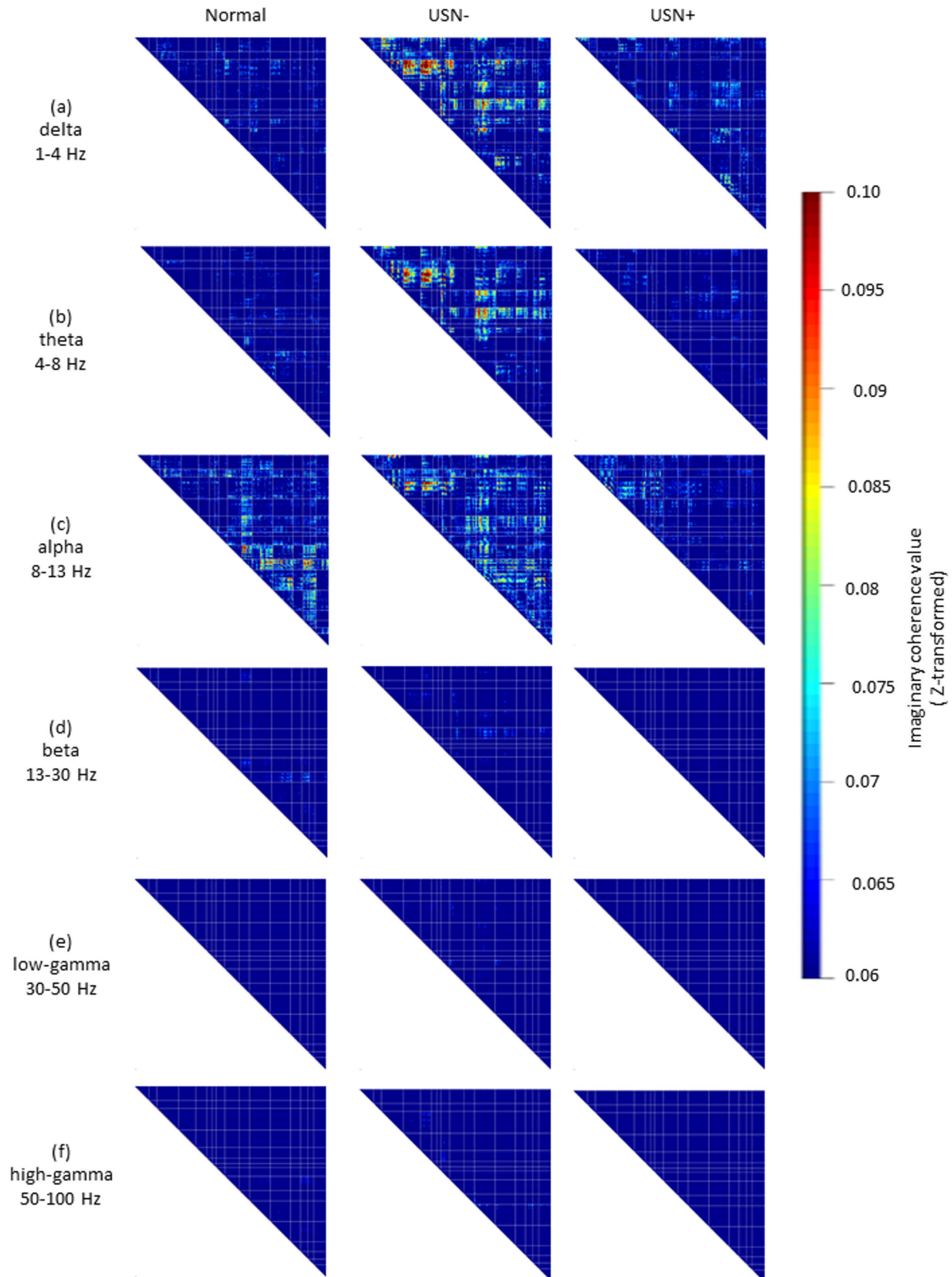**Figure 3. IC matrices among groups at each frequency band.** The patterns of IC matrices in the delta (a) and theta band (b) were similar. The matrices in the beta band (d) and low-/high-gamma (e, f) band were also similar. Unlike the IC matrices in other frequency bands, the IC matrices in the alpha band (c) were considerably different among the groups. The color scale indicates imaginary coherence value (Z-transformed).
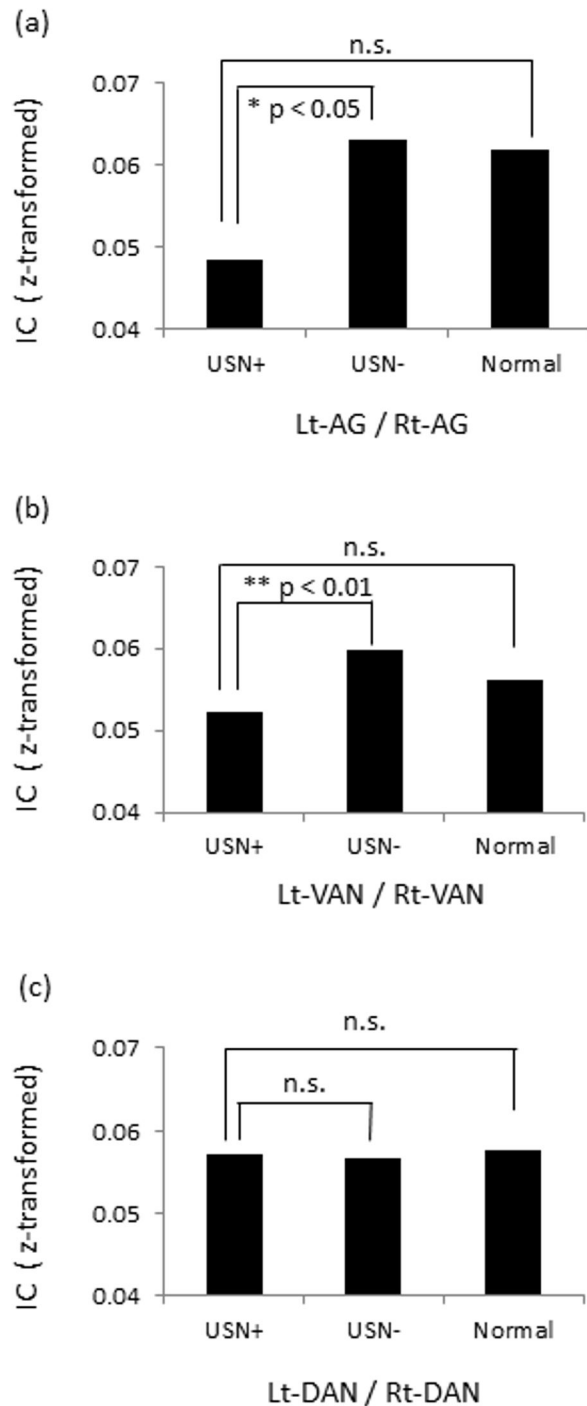
Figure 4. Comparisons of IC of inter-hemispheric attentional regions in the alpha band (8–13 Hz). (a) In left/right AG, the USN(+) group showed lower IC than the USN(-) group (uncorrected p < 0.05). (b) In left/right VAN, the USN(+) group showed lower IC than USN(-) (uncorrected p < 0.01). (c) In left/right DAN, no statistical difference was found among the groups.

interactions between the VAN and DAN. Finally, the occurrence of inter-hemispherical imbalance contributes to spatial neglect [24,25]. Based on these findings, the most plausible explanation of the present results may be that reduced connectivity through the corpus callosum between left and right AG [66] resulted in the dysfunction of the DAN; the impaired functioning of the DAN, in turn, interfered with patients' abilities to shift and maintain attention (i.e., spatial neglect).

One of the most fascinating results of this study is that the disturbed connectivity of the attentional network discussed above was most striking in the alpha band. Notably, patients with USN also showed lower inter-hemispherical connectivity of the VAN in the low-gamma band; however, the IC values in the low-gamma band were not correlated with USN severity. One reason for the strength of our observation in the alpha band is that the alpha band signal is robust during rest [53] and has the highest signal-to-noise ratio of all the frequency bands [67]. In addition, as demonstrated by Hinkley et al., reliability of measuring the alpha band signal is high both within-sessions and cross-sessions as compared to that of measuring signals at other frequency bands [68]. Furthermore, it has been hypothesized that the alpha band may play a role in attentional processing [69–71], the visual network [72], and in inter-hemispherical network balance [73]. On the other hand, it has been reported that the gamma band may play a role in network modulation in the active condition [74,75], whereas slow waves, including those in the delta and theta range, may be followed by brain damage itself [76,77]. Accordingly, we can infer that the alpha band IC between the left and right VAN, especially in the AG, could be one of the biomarkers of attentional network imbalance occurring in patients with USN.

Our results are also consistent with previous findings that spontaneous neural activity at rest predicts clinical variables such as epilepsy [1], depression [2], schizophrenia [3], dementia [4], and autism [5]. Resting functional connectivity relates not only to symptoms, but also to task performance dedicated to a given cognitive function [78–80]. As pointed out in Rosazza et al. [81], resting neural activity consumes the majority of brain energy [82] and supports neural signaling processes subserving the integration of information originating from internal as well as external phenomena. With respect to the present results, a change in baseline communication, in the left/right VAN, especially in the alpha band, may significantly affect the way these regions are recruited and how they communicate in a range of situations.

Although the small size of our subject cohort may limit the statistical power of our results, we feel confident in concluding that disturbed alpha band left/right VAN connectivity, especially in the AG, is correlated with severity of USN symptoms. However, considering that individual variations of functional network in healthy subjects [25] and of brain activities in patients with USN [83], it is obvious that we should collect data from additional subjects with and without USN as well as age-matched healthy controls to elaborate present findings. Another limitation of this study is that we did not focus on the networks other than attentional networks. Therefore, we could not specify the network unrelated to attentional control as well as
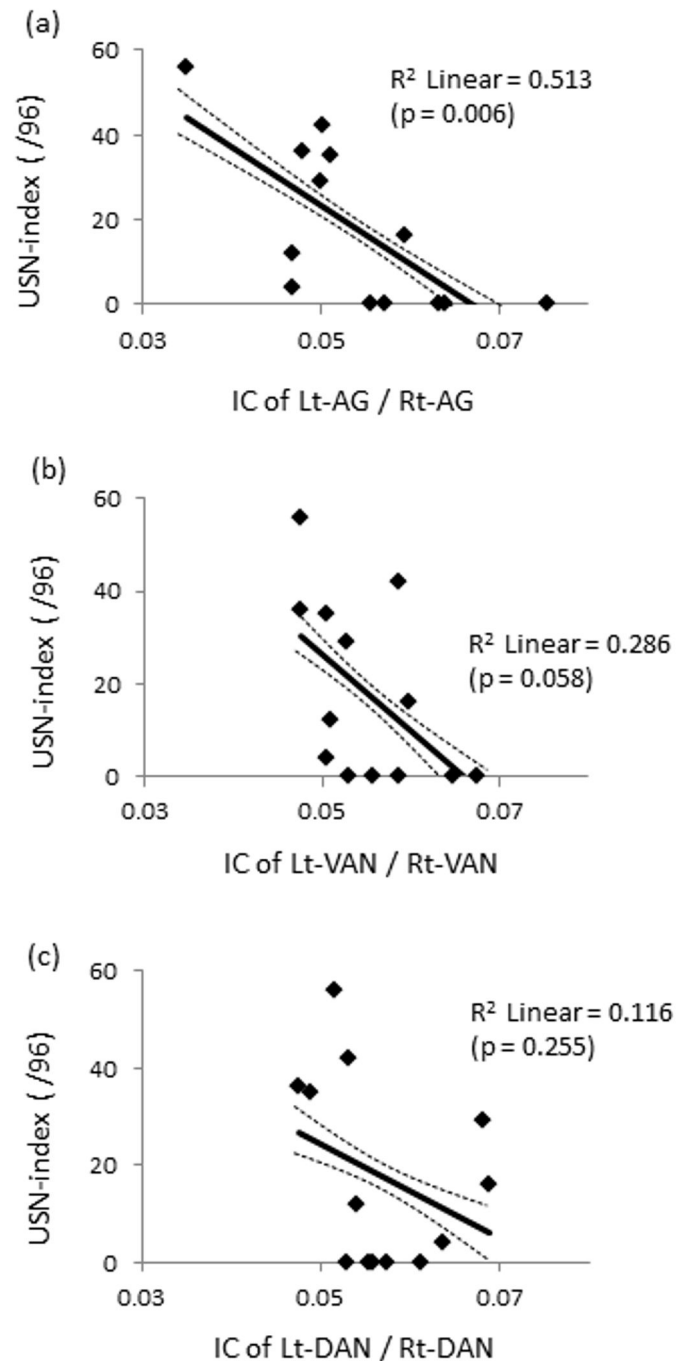
Figure 5. Correlations between imaginary coherence and USN index in the alpha band (8–13 Hz). Scatter plot of data for 13 patients with brain damage. (a) A significant correlation with IC of the left/right AG and USN index was found ($F_{(1,11)}$ = 11.597, p = 0.006, r^2 = 0.513). (b) A correlation with IC of the left/right VAN and USN index showed a trend for significance ($F_{(1,11)}$ = 4.403, p = 0.058, r^2 = 0.286). (c) but no significance was found in the left/right DAN ($F_{(1,11)}$ = 1.442, p = 0.255, r^2 = 0.116). The solid line and dotted line represents regression line, 95% confidence intervals for the line of best fit, respectively.
doi: 10.1371/journal.pone.0073416.g005

the relationship between these networks. Further study should address issues of interactions across bands, power analysis [35], non-stationary analysis [27], and network changes after treatment [84] with larger populations of subjects.

Supporting Information

Figure S1. Representations of position of 388 nodes. (a) top view, (b) front view, (c) back view, (d) left side view, (e) right side view. Light-blued dots represent SFG (superior frontal gyrus), dark-blue represents SPL (superior parietal lobule), blue represents MT (middle temporal region). Red, orange, pink, yellow, and green represents VFG (ventral frontal gyrus), IFG (inferior frontal gyrus), AG (angular gyrus), SMG (supramarginal gyrus), STG (superior temporal gyrus), respectively.
(TIF)

Table S1. The number of nodes (voxels) in each ROI. SFG: superior frontal gyrus; SPL: superior parietal lobule; MT: middle temporal region; VFG: ventral frontal gyrus; IFG: inferior frontal

gyrus; SMG: supramarginal gyrus; AG: angular gyrus; STG: superior temporal gyrus.
(DOCX)

Author Contributions

Conceived and designed the experiments: TS. Performed the experiments: TS MA TO KK WI HK. Analyzed the data: TS EO KS. Wrote the manuscript: TS EO.

References

1. Pittau F, Grova C, Moeller F, Dubeau F, Gotman J (2012) Patterns of altered functional connectivity in mesial temporal lobe epilepsy. Epilepsia 53: 1013-1023. doi:10.1111/j.1528-1167.2012.03464.x. PubMed: 22578020.
2. Liu L, Zeng LL, Li Y, Ma Q, Li B et al. (2012) Altered cerebellar functional connectivity with intrinsic connectivity networks in adults with major depressive disorder. PLOS ONE 7: e39516. doi:10.1371/journal.pone.0039516. PubMed: 22724025.
3. Meda SA, Gill A, Stevens MC, Lorenzoni RP, Glahn DC et al. (2012) Differences in resting-state functional magnetic resonance imaging functional network connectivity between schizophrenia and psychotic bipolar probands and their unaffected first-degree relatives. Biol Psychiatry 71: 881-889. doi:10.1016/j.biopsych.2012.01.025. PubMed: 22401986.
4. Brier MR, Thomas JB, Snyder AZ, Benzinger TL, Zhang D et al. (2012) Loss of intranetwork and internetwork resting state functional connections with Alzheimer's disease progression. J Neurosci 32: 8890-8899. doi:10.1523/JNEUROSCI.5698-11.2012. PubMed: 22745490.
5. Tsiaras V, Simos PG, Rezaie R, Sheth BR, Garyfallidis E et al. (2011) Extracting biomarkers of autism from MEG resting-state functional connectivity network. Comput Biol Med 41: 1166-1177. doi:10.1016/j.compbiomed.2011.04.004. PubMed: 21592470.
6. Meunier D, Achard S, Morcom A, Bullmore E (2009) Age-related changes in modular organization of human brain functional networks. NeuroImage 44: 715-723. doi:10.1016/j.neuroimage.2008.09.062. PubMed: 19027073.
7. Bonnelle V, Leech R, Kinnunen KM, Ham TE, Beckmann CF et al. (2011) Default mode network connectivity predicts sustained attention deficits after traumatic brain injury. J Neurosci 31: 13442-13451. doi:10.1523/JNEUROSCI.1163-11.2011. PubMed: 21940437.
8. Wang L, LaViolette P, O'Keefe K, Putcha D, Bakkour A et al. (2010) Intrinsic connectivity between the hippocampus and posteromedial cortex predicts memory performance in cognitively intact older individuals. NeuroImage 51: 910-917. doi:10.1016/j.neuroimage.2010.02.046. PubMed: 20188183.
9. Sun YW, Qin LD, Zhou Y, Xu Q, Qian LJ et al. (2011) Abnormal functional connectivity in patients with vascular cognitive impairment, no dementia: A resting-state functional magnetic resonance imaging study. Behav Brain Res 223: 388-394. doi:10.1016/j.bbr.2011.05.006. PubMed: 21605598.
10. Buxbaum LJ, Ferraro MK, Veramonti T, Farne A, Whyte J et al. (2004) Hemispatial neglect: Subtypes, neuroanatomy, and disability. Neurology 62: 749–756. doi:10.1212/01.WNL.0000113730.73031.F4. PubMed: 15007125.
11. Appelros P, Karlsson GM, Seiger A, Nydevik I (2002) Neglect and anosognosia after first-ever stroke: Incidence and relationship to disability. J Rehabil Med 34: 215–220. doi:10.1080/165019702760279206. PubMed: 12392236.
12. Heilman KM, Watson RT, Bower D, Valenstein E (1983) Right hemisphere dominance for attention. Rev Neurol 25: 3161-3167.
13. Vallar G (2001) Extrapersonal visual unilateral spatial neglect and its neuroanatomy. Neuroimage 14: 52-58. doi:10.1006/nimg.2001.0822. PubMed: 11373133.
14. Doricchi F, Tomaiuolo F (2003) The anatomy of neglect without hemianopia: a key role for parietal-frontal disconnection? Neuroreport 14: 2239-2243. doi:10.1097/00001756-200312020-00021. PubMed: 14625455.
15. Hillis AE, Newhart M, Heidler J, Barker PB, Herskovits EH et al. (2005) Anatomy of spatial attention: insights from perfusion imaging and hemispatial neglect in acute stroke. J Neurosci 25: 3161-3167. doi:10.1523/JNEUROSCI.4468-04.2005. PubMed: 15788773.
16. Husain M, Kennard C (1996) Visual neglect associated with frontal lobe infarction. J Neurol 243: 652-657. doi:10.1007/BF00878662. PubMed: 8892067.
17. Karnath HO, Ferber S, Himmelbach M (2001) Spatial awareness is a function of the temporal not the posterior parietal lobe. Nature 411: 950-953. doi:10.1038/35082075. PubMed: 11418859.
18. Cambier J, Masson M, Graveleau P, Elghozi D (1980) Symptomatology of neglect in ischemic lesions of the territory of the right posterior cerebral artery: Role of thalamic lesions. Rev Neurol 138: 631-348.
19. Vallar G, Perani D (1986) The anatomy of unilateral neglect after right hemisphere stroke lesions. A clinical/CT-scan correlation study in man. Neuropsychologia 24: 609-622. doi:10.1016/0028-3932(86)90001-1. PubMed: 3785649.
20. Healton EB, Navarro C, Bressman S, Brust JCM (1982) Subcortical neglect. Neurology 32: 776-778. doi:10.1212/WNL.32.7.776. PubMed: 7201116.
21. Karnath HO, Himmelbach M, Rorden C (2002) The subcortical anatomy of human spatial neglect: putamen, caudate nucleus and pulvinar. Brain 125: 350-360. doi:10.1093/brain/awf032. PubMed: 11844735.
22. Hildebrandt H, Spang K, Ebke M (2002) Visuospatial hemi-inattention following cerebellar/brain stem bleeding. Neurocase 8: 323-329. doi:10.1076/neur.8.3.323.16197. PubMed: 12221145.
23. Mesulam MM (1981) A cortical network for directed attention and unilateral neglect. Ann Neurol 10: 309-325. doi:10.1002/ana.410100402. PubMed: 7032417.
24. Corbetta M, Shulman GL (2011) Spatial neglect and attention networks. Annu Rev Neurosci 34: 569-599. doi:10.1146/annurev-neuro-061010-113731. PubMed: 21692662.
25. Corbetta M (2012) Functional connectivity and neurological recovery. Dev Psychobiol 54: 239-253. doi:10.1002/dev.20507. PubMed: 22415913.
26. Fox MD, Corbetta M, Snyder AZ, Vincent JL, Raichle ME (2006) Spontaneous neural activity distinguishes human dorsal and ventral attention systems. Proc Natl Acad Sci U S A 103: 10046-10051. doi:10.1073/pnas.0604187103. PubMed: 16788060.
27. de Pasquale F, Penna SD, Snyder AZ, Lewis C, Mantini D et al. (2010) Temporal dynamics of spontaneous MEG activity in brain networks. Proc Natl Acad Sci U S A 107: 6040-6045. doi:10.1073/pnas.0913863107. PubMed: 20304792.
28. Bartolomeo P (2006) A parietofrontal network for spatial awareness in the right hemisphere of the human brain. Arch Neurol 63: 1238-1241. doi:10.1001/archneur.63.9.1238. PubMed: 16966500.

29. Urbanski M, Thiebaut de Schotten M, Rodrigo S, Oppenheim C, Touzé E et al. (2010) DTI-MR tractography of white matter damage in stroke patients with neglect. Exp Brain Res 208: 491-505. PubMed: 21113581.

30. He BJ, Snyder AZ, Vincent JL, Epstein A, Shulman GL et al. (2007) Breakdown of functional connectivity in frontoparietal networks underlies behavioral deficits in spatial neglect. Neuron 53: 905-918. doi: 10.1016/j.neuron.2007.02.013. PubMed: 17359924.

31. Corbetta M, Kincade MJ, Lewis C, Snyder AZ, Sapir A (2005) Neural basis and recovery of spatial attention deficits in spatial neglect. Nat Neurosci 8: 1603-1610. doi:10.1038/nn1574. PubMed: 16234807.

32. Carter AR, Astafiev SV, Lang CE, Connor LT, Rengachary J et al. (2010) Resting interhemispheric functional magnetic resonance imaging connectivity predicts performance after stroke. Ann Neurol 67: 365-375. PubMed: 20373348.

33. Logothetis NK (2008) What we can do and what we cannot do with fMRI. Nature 453: 869-878. doi:10.1038/nature06976. PubMed: 18548064.

34. Siegel M, Donner TH, Engel AK (2012) Spectral fingerprints of large-scale neuronal interactions. Nat Rev Neurosci 13: 121-134. PubMed: 22233726.

35. Hipp JF, Hawellek DJ, Corbetta M, Siegel M, Engel AK (2012) Large-scale cortical correlation structure of spontaneous oscillatory activity. Nat Neurosci 15: 884-890. doi:10.1038/nn.3101. PubMed: 22561454.

36. Doesburg SM, Vinette SA, Cheung MJ, Pang EW (2012) Theta-modulated gamma-band synchronization among activated regions during a verb generation task. Front Psychol 3: 195. PubMed: 22707946.

37. Westlake KP, Hinkley LB, Bucci M, Guggisberg AG, Findlay AM et al. (2012) Resting state functional connectivity and recovery after stroke. Exp Neurol 237: 160-169. doi:10.1016/j.expneurol.2012.06.020. PubMed: 22750324.

38. Oldfield RC (1971) The assessment and analysis of handedness: The Edinburgh Inventory. Neuropsychologia 9: 97-113. doi: 10.1016/0028-3932(71)90067-4. PubMed: 5146491.

39. Folstein MF, Folstein SE, McHugh PR (1975) "Mini-mental state." A practical method for grading the cognitive state of patients for the clinician. J Psychiatr Res 12: 189-198. doi: 10.1016/0022-3956(75)90026-6. PubMed: 1202204.

40. Behavioural inattention test©, Japanese edition (1999) Shinkoh Igaku Shuppan Co., LTD: Tokyo, Japan.

41. Azouvi P, Olivier S, de Montety G, Samuel C, Louis-Dreyfus A et al. (2003) Behavioral assessment of unilateral neglect: study of the psychometric properties of the Catherine Bergego Scale. Arch Phys Med Rehabil 84: 51-57. PubMed: 12589620.

42. Rorden C, Brett M (2000) Stereotaxic display of brain lesions. Behav Neurol 12: 191-200. PubMed: 11568431.

43. Oostenveld R, Fries P, Maris E, Schoffelen JM (2011) FieldTrip: Open source software for advanced analysis of MEG, EEG, and invasive electrophysiological data. Comput Intell Neurosci 2011. Available: http://www.hindawi.com/journals/cin/2011/156869. Accessed 15 August 2013.

44. Maldjian JA, Laurienti PJ, Kraft RA, Burdette JH (2003) An automated method for neuroanatomic and cytoarchitectonic atlas-based interrogation of fMRI data sets. Neuroimage 19: 1233-1239. PubMed: 12880848.

45. Maldjian JA, Laurienti PJ, Burdette JH (2004) Precentral gyrus discrepancy in electronic versions of the Talairach Atlas. Neuroimage 21: 450-455. PubMed: 14741682.

46. Tzourio-Mazoyer N, Landeau B, Papathanassiou D, Crivello F, Etard O et al. (2002) Automated anatomical labeling of activations in SPM using a macroscopic anatomical parcellation of the MNI MRI single-subject brain. Neuroimage 15: 273-289. PubMed: 11771995.

47. Nolte G, Bai O, Wheaton L, Mari Z, Vorbach S et al. (2004) Identifying true brain interaction from EEG data using the imaginary part of coherency. Clin Neurophysiol 115: 2292-2307. PubMed: 15351371.

48. Sekihara K, Owen JP, Trisno S, Nagarajan SS (2011) Removal of spurious coherence in MEG source-space coherence analysis. IEEE Trans Biomed Eng 58: 3121-3129. PubMed: 21824842.

49. Martino J, Honma SM, Findlay AM, Guggisberg AG, Owen JP et al. (2011) Resting functional connectivity in patients with brain tumors in eloquent areas. Ann Neurol 69: 521-532. doi:10.1002/ana.22167. PubMed: 21400562.

50. Sekihara K, Nagarajan SS (2008) Adaptive spatial filters for electromagnetic brain imaging. Springer-Verlag. 245pp.

51. Carlson BD (1988) Covariance matrix estimation errors and diagonal loading in adaptive arrays. IEEE Trans Aerosp Electron Syst 24: 397–401. doi:10.1109/7.7181.

52. Cox H, Zeskind RM, Owen MM (1987) Robust adaptive beamforming. IEEE Trans Signal Process 35: 1365–1376.

53. Guggisberg AG, Honma SM, Findlay AM, Dalal SS, Kirsch HE et al. (2008) Mapping functional connectivity in patients with brain lesions. Ann Neurol 63: 193-203. doi:10.1002/ana.21224. PubMed: 17894381.

54. Siegel M, Donner TH, Oostenveld R, Fries P, Engel AK (2008) Neuronal synchronization along the dorsal visual pathway reflects the focus of spatial attention. Neuron 60: 709-719. doi:10.1016/j.neuron.2008.09.010. PubMed: 19038226.

55. Liu Z, Fukunaga M, de Zwart JA, Duyn JH (2010) Large-scale spontaneous fluctuations and correlations in brain electrical activity observed with magnetoencephalography. NeuroImage 51: 102-111. doi:10.1016/j.neuroimage.2010.01.092. PubMed: 20123024.

56. Castellanos NP, Leyva I, Buldú JM, Bajo R, Paúl N et al. (2011) Principles of recovery from traumatic brain injury: Reorganization of functional networks. NeuroImage 55: 1189-1199. doi:10.1016/j.neuroimage.2010.12.046. PubMed: 21195199.

57. Douw L, Schoonheim MM, Landi D, van der Meer ML, Geurts JJG et al. (2011) Cognition is related to resting-state small-world network topology: An magnetoencephalographic study. Neurosci 175: 169-177. PubMed: 21130847.

58. Shulman GL, Astafiev SV, Franke D, Pope DL, Snyder AZ et al. (2009) Interaction of stimulus-driven reorienting and expectation in ventral and dorsal frontoparietal and basal ganglia-cortical networks. J Neurosci 29: 4392-4407. doi:10.1523/JNEUROSCI.5609-08.2009. PubMed: 19357267.

59. Corbetta M, Shulman GL (2002) Control of goal-directed and stimulus-driven attention in the brain. Nat Rev Neurosci 3: 201-215. PubMed: 11994752.

60. Silver MA, Ress D, Heeger DJ (2005) Topographic maps of visual spatial attention in human parietal cortex. J Neurophysiol 94: 1358-1371. doi:10.1152/jn.01316.2004. PubMed: 15817643.

61. Malhotra P, Coulthard E, Husain M (2006) Hemispatial neglect, balance and eye-movement control. Curr Opin Neurol 19: 14-20. doi: 10.1097/01.wco.0000198101.87670.7e. PubMed: 16415672.

62. Milner AD, McIntosh RD (2005) The neurological basis of visual neglect. Curr Opin Neurol 18: 748-753. doi:10.1097/01.wco.0000191512.60368.ee. PubMed: 16280689.

63. Husain M, Rorden C (2003) Non-spatially lateralized mechanisms in hemispatial neglect. Nat Rev Neurosci 4: 26-36. doi:10.1038/nrn1005. PubMed: 12511859.

64. Malhotra P, Coulthard EJ, Husain M (2009) Role of right posterior parietal cortex in maintaining attention to spatial locations over time. Brain 132: 645-660. doi:10.1093/brain/awn350. PubMed: 19158107.

65. Rengachary J, He BJ, Shulman GL, Corbetta M (2011) A behavioral analysis of spatial neglect and its recovery after stroke. Front Hum Neurosci 5: 1-13. PubMed: 21283556.

66. Schulte T, Müller-Oehring EM (2010) Contribution of callosal connections to the interhemispheric integration of visuomotor and cognitive processes. Neuropsychol Rev 20: 174-190. doi:10.1007/s11065-010-9130-1. PubMed: 20411431.

67. Nunez PL, Wingeier BM, Silberstein RB (2001) Spatial-temporal structures of human alpha rhythms: theory, microcurrent sources, multiscale measurements, and global binding of local networks. Hum Brain Mapp 13: 125-164. doi:10.1002/hbm.1030. PubMed: 11376500.

68. Hinkley LB, Vinogradov S, Guggisberg AG, Fisher M, Findlay AM et al. (2011) Clinical symptoms and alpha band resting-state functional connectivity imaging in patients with schizophrenia: implications for novel approaches to treatment. Biol Psychiatry 70: 1134-1142. doi: 10.1016/j.biopsych.2011.06.029. PubMed: 21861988.

69. Klimesch W (1999) EEG alpha and theta oscillations reflect cognitive and memory performance: a review and analysis. Brain Res Rev 29: 169-195. doi:10.1016/S0165-0173(98)00056-3. PubMed: 10209231.

70. Hirschmann J, Özkurt TE, Butz M, Homburger M, Elben S et al. (2011) Distinct oscillatory STN-cortical loops revealed by simultaneous MEG and local field potential recordings in patients with Parkinson's disease. NeuroImage 55: 1159-1168. doi:10.1016/j.neuroimage.2010.11.063. PubMed: 21122819.

71. Litvak V, Jha A, Eusebio A, Oostenveld R, Foltynie T et al. (2011) Resting oscillatory cortico-subthalamic connectivity in patients with Parkinson's disease. Brain 134: 359-374. doi:10.1093/brain/awq332. PubMed: 21147836.

72. Scheeringa R, Petersson KM, Kleinschmidt A, Jensen O, Bastiaansen MC (2012) EEG alpha power modulation of FMRI resting-state connectivity. Brain Connect 2: 254-264. doi:10.1089/brain.2012.0088. PubMed: 22938826.

73. Westlake KP, Hinkley LB, Bucci M, Guggisberg AG, Byl N et al. (2012) Resting state α-band functional connectivity and recovery after stroke.

Exp Neurol 237: 160-169. doi:10.1016/j.expneurol.2012.06.020. PubMed: 22750324.

74. Buschman TJ, Miller EK (2007) Top-down versus bottom-up control of attention in the prefrontal and posterior parietal cortices. Science 315: 1860-1862. doi:10.1126/science.1138071. PubMed: 17395832.

75. Doesburg SM, Vinette SA, Cheung MJ, Pang EW (2012) Theta-modulated gamma-band synchronization among activated regions during a verb generation task. Front Psychol 3: 195. PubMed: 22707946.

76. Butz M, Gross J, Timmermann L, Moll M, Freund HJ et al. (2004) Perilesional pathological oscillatory activity in the magnetoencephalogram of patients with cortical brain lesions. Neurosci Lett 355: 93-96. doi:10.1016/j.neulet.2003.10.065. PubMed: 14729243.

77. Sakamoto S, Tanaka H, Tsuyuguchi N, Terakawa Y, Ohata K et al. (2010) Quantitative imaging of spontaneous neuromagnetic activity for assessing cerebral ischemia using sLORETA-qm. Neuroimage 49: 488-497. doi:10.1016/j.neuroimage.2009.07.039. PubMed: 19632340.

78. Hampson M, Driesen NR, Skudlarski P, Gore JC, Constable RT (2006) Brain connectivity related to working memory performance. J Neurosci

26: 13338-13343. doi:10.1523/JNEUROSCI.3408-06.2006. PubMed: 17182784.

79. Fox MD, Snyder AZ, Vincent JL, Raichle ME (2007) Intrinsic fluctuations within cortical systems account for intertribal variability in human behavior. Neuron 56: 171-184. doi:10.1016/j.neuron. 2007.08.023. PubMed: 17920023.

80. Hasson U, Nusbaum HC, Small SL (2009) Task-dependent organization of brain regions active during rest. Proc Natl Acad Sci USA 106: 10841-10846. doi:10.1073/pnas.0903253106. PubMed: 19541656.

81. Rosazza C, Minati L (2011) Resting-state brain networks: literature review and clinical applications. Neurol Sci 32: 773-785. doi:10.1007/s10072-011-0636-y. PubMed: 21667095.

82. Raichle ME, Mintun MA (2006) Brain work and brain imaging. Annu Rev Neurosci 29: 449-476. doi:10.1146/annurev.neuro. 29.051605.112819. PubMed: 16776593.

83. Mizuno K, Tsuji T, Masakado Y, Ota T, Honaga K et al. (2005) Visual evoked fields in patients of unilateral spatial neglect. Int Congr Ser 1278: 215-218. doi:10.1016/j.ics.2004.11.078.

84. Oliveri M (2011) Brain stimulation procedures for treatment of contralesional spatial neglect. Restor Neurol Neurosci 29: 421-425. PubMed: 22124030.